

Positron emission tomographic measurement of blood-to-brain and blood-to-tumour transport of ^{82}Rb . I: Error analysis and computer simulations

Vijay Dhawan‡, Alexander Poltorak, James R Moeller, Jens O Jarden
Stephen C Strother, Howard Thaler† and David A Rottenberg

Department of Neurology and † Department of Biostatistics, Memorial Sloan-Kettering
Cancer Center, 1275 York Avenue, New York, NY 10021, USA

Abstract. Unidirectional blood-to-brain and blood-to-tumour transport rate constants (K_1) for ^{82}Rb (half-life 76 s) and plasma water volume per unit mass of brain/tumour tissue (V_p) can be estimated *in vivo* using dynamic positron emission tomography (PET). The accuracy of these estimates depends upon the accuracy of PET measurements of regional brain/tumour radioactivity and scintillation well detector measurements of whole-blood radioactivity, which, in turn, depend upon the time course of arterial blood radioactivity. A two-compartmental model has been employed to derive estimates for K_1 , k_2 (efflux rate constant) and V_p from ^{82}Rb /PET data. Errors in these parameter estimates have been studied (1) qualitatively using sensitivity function analysis and (2) quantitatively using computer simulations. The effect of adding a third irreversible compartment and its unidirectional rate constant, k_3 , has also been investigated. The advantages and disadvantages of bolus injection vs continuous infusion protocols are discussed. Precision in estimated parameters from actual patient data is compared to that obtained from computer simulations in part II of this paper.

1. Introduction

Several recent publications have discussed the application of positron emission tomography (PET) to the quantitative study of blood-brain barrier (BBB) integrity using short-lived positron emitters such as ^{68}Ga (as $^{68}\text{Ga-EDTA}$), $^{13}\text{NH}_3$ and ^{82}Rb (Blasberg *et al* 1984, Hawkins *et al* 1984, Kessler *et al* 1984, Lockwood 1984, Brooks *et al* 1984, Lammertsma *et al* 1984, Takagi *et al* 1984, Jarden *et al* 1984, 1985). Blasberg *et al* (1984) published preliminary estimates of the blood-to-brain and blood-to-tumour transport rate constants for $^{68}\text{Ga-EDTA}$ in beagle dogs with avian sarcoma virus-induced brain tumours and derived estimates of the initial/vascular volume for both tumour and normal brain tissue. Hawkins *et al* (1984) employed the same tracer and a two-compartment tracer kinetic model to evaluate BBB permeability in 12 patients with primary and metastatic brain tumours. Quantitative measurements of BBB permeability using ^{82}Rb /PET have also been reported by Brooks *et al* (1984); these authors derived estimates of the regional extraction of ^{82}Rb using a steady-state model involving the sequential administration of ^{82}Rb (continuous intravenous infusion), CO^{15}O (continuous inhalation) and ^{11}CO (bolus inhalation). An error analysis of this multiple-studies approach has been published by Lammertsma *et al* (1984) and Takagi *et al* (1984). Lammertsma's (1984) approach to the measurement of regional ^{82}Rb extraction fraction requires three separate PET studies and is associated with an overall uncertainty of 10% for brain tumours.

‡ Present address: North Shore University Hospital, Cornell University Medical College, NY, USA

Our interest in the rapid temporal effect of pharmacological (steroids) intervention on the blood-tumour barrier prompted us to investigate a short bolus protocol to obtain the unidirectional influx transport rate constant (K_1) for ^{82}Rb *in vivo*. If it can be assumed that the regional cerebral blood flow remains constant and is not extremely low (i.e. $<5 \text{ ml min}^{-1} 100 \text{ g}^{-1}$), then K_1 approximates the permeability-surface area product (ps) for Rb with an error of $<6\%$ (Blasberg *et al* 1983a, Jarden *et al* 1985). The assumption of constant flow is more likely to be valid during a short bolus study than during a 15–20 min constant infusion protocol.

In a previous paper (Jarden *et al* 1985), we reported the results of ^{82}Rb /PET studies of patients with primary and metastatic brain tumours before and after whole-brain radiation therapy (WBRT) and/or dexamethasone treatment. These studies, undertaken in an effort to quantitate radiation and steroid-induced changes in BBB and blood-tumour barrier permeability, also provided estimates of brain and tumour plasma volume. The present communication describes an error analysis of the double-integral method proposed by Jarden *et al* (1985) and compares the accuracy of parameter estimates obtained with bolus injection and continuous infusion protocols.

We have also investigated the effect of several experimental and physiological variables on the parameter estimates. The experimental variables include (1) time shift between blood and brain radioactivity curves, (2) amount of ^{82}Rb injected and (3) number of PET scans. An important physiological variable is tissue heterogeneity, which cannot be controlled but (in a non-linear model) may lead to overestimates or underestimates of the true composite parameter value (Herscovitch and Raichle 1983). The effect of neglecting Rb backflux (k_2), the effect of ^{82}Rb uptake into the red blood cells (RBC) during the study period and the effect of extending the model to include a third irreversible compartment, k_3 , have also been investigated. The effect of time-shift and blood curve waveform smearing have been dealt with in detail elsewhere (Dhawan *et al* 1988).

2. Theory

A simple two-compartment model adequately describes the passive exchange of ^{82}Rb between arterial plasma and brain tissue (figure 1). This exchange can be described mathematically by the following equations

$$dA_t(t)/dt = K_1 C_p(t) - k_2 A_t(t) - \alpha A_t(t) \quad (1)$$

$$A_m(t) = A_t(t) + V_p C_p(t), \quad (2)$$

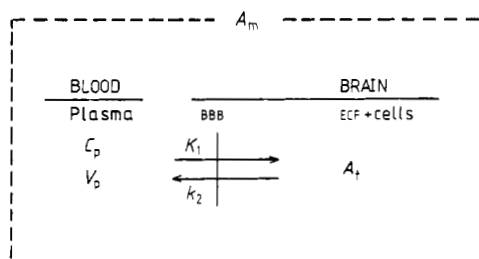


Figure 1. Two-compartment model of the blood-to brain transport of ^{82}Rb . C_p is plasma ^{82}Rb concentration (Ci ml^{-1}), A_t is extravascular brain tissue ^{82}Rb concentration (Ci g^{-1}), V_p is tissue plasma water volume (ml g^{-1}) and K_1 ($\text{ml min}^{-1} \text{g}^{-1}$) and k_2 (min^{-1}) represent influx and efflux rate constants. A_m is tissue concentration as measured by PET, i.e. extravascular and intravascular label.

where $A_i(t)$ is instantaneous extravascular brain tissue ^{82}Rb activity (Ci g^{-1}), $A_m(t)$ is brain tissue ^{82}Rb activity (Ci g^{-1}) as measured by PET (i.e. including intravascular label), $C_p(t)$ is instantaneous plasma ^{82}Rb activity (Ci ml^{-1}), K_1 is the influx rate constant ($\text{ml min}^{-1} \text{g}^{-1}$), k_2 is the efflux rate constant (min^{-1}), V_p is tissue plasma water volume (ml g^{-1}) and α is the decay constant for ^{82}Rb (0.547 min^{-1}). T_1 and T_2 are scan start and end times in minutes. Equation (2) is valid when red cell uptake is negligible. If red cell uptake cannot be neglected, it can be accounted for by replacing $V_p C_p$ by $V_b C_b$, where $C_b(t)$ is instantaneous blood water ^{82}Rb activity (Ci ml^{-1}), and V_b is whole-blood water volume (ml g^{-1}).

Based on these relationships, one can derive an operational equation which permits the estimation of K_1 , k_2 and V_p from PET region-of-interest (ROI) data and the time course of blood ^{82}Rb radioactivity

$$A = \int_{T_1}^{T_2} A_m(t) dt = K_1 \int_{T_1}^{T_2} e^{-k_2' t} \int_0^t C_p(u) e^{k_2' u} du dt + \int_{T_1}^{T_2} V_p C_p(t) dt, \quad (3)$$

where $k_2' = k_2 + \alpha$.

Quantitative error analysis of the model can be performed through computer simulations by adding noise to the measured variables in equation (3) and then using a non-linear regression algorithm to estimate the model parameters. There also exists a simple analytical tool (sensitivity function (SF) analysis, Huang and Phelps 1985) for providing a qualitative description of the ability of the model to extract parameter estimates under different experimental conditions. The magnitude of the SF curve for a particular parameter reflects the sensitivity of the measured variable to a small change in that parameter. The shape of the SF curve, on the other hand, provides information about the relative sensitivity of the primary output variable (e.g. A_m) to a change in the model parameter of interest during different phases of the study. This analytical method is implemented by taking the partial derivatives of A_m (instantaneous form of equation (3), i.e. without the integration from T_1 to T_2) with respect to the three parameters (K_1 , k_2 and V_p).

3. Methods

The range of parameter values used for SF analysis and computer simulations were obtained from our previously published clinical data (Jarden *et al* 1985). These ranges for K_1 and V_p were: $0.001 < K_1 < 0.1 \text{ ml min}^{-1} \text{g}^{-1}$ and $0.03 < V_p < 0.07 \text{ ml g}^{-1}$, respectively. k_2 was allowed to vary over a wide range, $0.1 K_1$ to $1.0 K_1$ †. Each study consisted of six 1 min scans. Simulated plasma activity curves were generated for both bolus and steady-state protocols assuming equal injected radioactivity (figure 2). Typical values of K_1 and V_p for tumour tissue were $0.09 \text{ ml min}^{-1} \text{g}^{-1}$ and 0.04 ml g^{-1} , respectively, and the corresponding values for normal brain were $0.007 \text{ ml min}^{-1} \text{g}^{-1}$ and 0.03 ml g^{-1} .

3.1. SF analysis

According to the procedure outlined in § 2, SF curves were computed using typical tumour and normal brain tissue parameter values and simulated plasma radioactivity profiles.

† Strictly speaking, this range represents only the magnitude of k_2 , since K_1 and k_2 have different units.

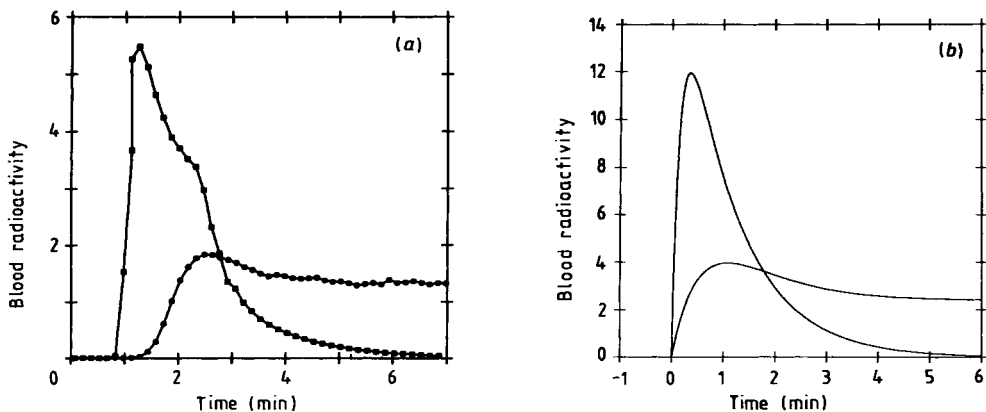


Figure 2. (a) Time course of blood ^{82}Rb activity following bolus injection (■) or continuous infusion (●) of tracer from the Squibb $^{82}\text{Sr}/^{82}\text{Rb}$ generator. Blood radioactivity in arbitrary units is plotted as a function of time. Blood sampling interval was 9 s. (b) Simulated blood radioactivity curves, $C_p(t)$, for the bolus injection and constant infusion protocol with equal injected radioactivity.

3.2. Computer simulations

In order to obtain a quantitative estimate of the magnitude of the error in K_1 , k_2 and V_p , computer simulations were performed over the above mentioned parameter ranges. Integrated brain activity was calculated at 1 min intervals from equation (3), which was solved for K_1 , k_2 and V_p using a non-linear regression routine, and the estimates thus obtained were compared with the actual parameter values. Gaussian noise was added to calculated regional brain activity. The coefficient of variation (cv) in A_m for the last 1 min scan was assumed to be 5–10% for bolus protocol, and the cv in A_m for other scans was scaled according to count rate in the following manner: $\text{cv}(A_m) = \% e \sqrt{[A_{\min}/A_m]}$, where e is either 5% or 10% cv in the last scan for the bolus protocol, and A_{\min} is the integrated brain activity for the same last scan. The assumed $\text{cv}(A_m)$ was based upon the experimental data of Jarden *et al* (1985): each 1 min image contained $>100\,000$ total coincidence counts, the tumour-to-brain count rate ratio was >5.0 , and the tumours (which were well defined and ranged from 3–10 cm^2 in cross-sectional area) included less than 10% of total slice area (Budinger *et al* 1978). Blood radioactivity can be determined with high precision ($<1\%$ error), and the error in $C_p(t)$ has therefore been neglected in this analysis. Other variables that can influence parameter estimates were individually analysed through computer simulations in the following manner:

(1) Count rate: amount of injected radioactivity (different count rate for the same scanning protocol). The magnitude of simulated blood curves was scaled by 0.5 and 0.25 to represent 60 and 30 mCi, respectively, of ^{82}Rb infused;

(2) Tissue heterogeneity: A_m for 'mixed' tissue was generated using weighted contributions from tumour and normal tissue for eight different weighting combinations (% tumour weight: 100, 80, 60, 40, 20, 10, 5, 0). Parameters estimated from these data sets were compared with the true parameter values of the composite tissue calculated as

$$P_c = w_t P_t + (1 - w_t) P_n, \quad (8)$$

where w_t is the fractional weight for tumour tissue, P_t and P_n are typical values for

tumour tissue and normal brain, and P_c is the corresponding value for composite tissue (equivalent homogeneous region). P may represent K_1 , k_2 or V_p .

(3) Number of scans/scan intervals: the brain curve was sampled more finely by increasing the number of scans to 12, each of 30 s duration.

For each of the above three conditions, simulations were performed over the specified range of parameter values. Precision in the estimated parameters was investigated by calculating the CV as

$$\% \text{ CV} = \frac{\text{one standard deviation in } \hat{p}}{p} \times 100,$$

where \hat{p} is the estimate of true parameter value p .

4. Results

4.1. Sensitivity function curves

4.1.1. Bolus injection. Figures 3(a, b) illustrate SF curves for the bolus injection case for tumour tissue when $k_2 = K_1$ and $k_2 = 0.1 K_1$, respectively. Figures 3(c, d) are the corresponding SF curves for normal brain. The SF curve for K_1 shows a sharp decrease in magnitude as K_1 is reduced from 0.09 (tumour) to 0.007 (normal brain). The SF curves for V_p closely follow the general shape of $C_p(t)$ (cf. figure 2(b) for tumour tissue and normal brain, irrespective of the value of k_2 . The effect of k_2 increases slowly with time but is clearly distinct from the zero axis only for the tumour case when $k_2 = K_1$.

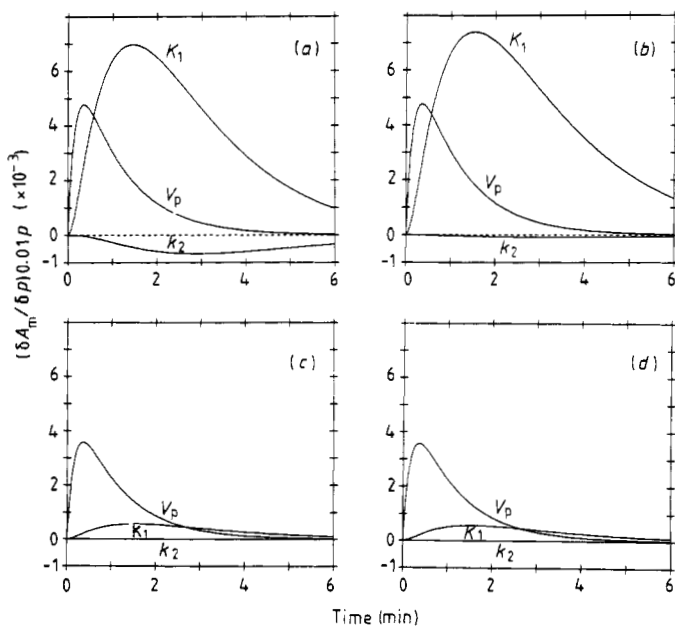


Figure 3. Sensitivity function curves (see text) for bolus injection protocol. (a) Tumour: $K_1 = k_2 = 0.09$, $V_p = 0.04$; (b) Tumour: $K_1 = 0.09$, $k_2 = 0.009$, $V_p = 0.04$; (c) Normal: $K_1 = k_2 = 0.007$, $V_p = 0.03$; (d) Normal: $K_1 = 0.007$, $k_2 = 0.0007$, $V_p = 0.03$. The units of y-axis are the same as for A_m .

4.1.2. *Constant infusion.* Figures 4(a, b) illustrate SF curves for the constant infusion protocol for tumour tissue when $k_2 = K_1$ and $k_2 = 0.1 K_1$, respectively. Figures 4(c, d) are the corresponding SF curves for normal brain. These curves can be described in much the same way as those relating to the bolus injection protocol (see § 5).

4.2. Computer simulations

Results for the cases $k_2 = 0.1 K_1$ and $k_2 = K_1$ were similar, and, therefore, the presentation of the simulation results is confined to the case $k_2 = 0.1 K_1$. Figures 5-7 were constructed from five discrete points, which correspond to K_1 values of 0.1, 0.05, 0.01, 0.005 and 0.001. Typical values for tumour tissue and normal brain thus correspond to the first ($K_1 = 0.1$) and the fourth ($K_1 = 0.005$) data points.

4.2.1. *Bolus vs constant infusion.* Figure 5 illustrates the cv in the estimate of K_1 , $cv(\hat{K}_1)$, for both bolus and constant infusion protocols. For either protocol, $cv(\hat{K}_1)$ is $< 5\%$ for tumour tissue. For the bolus protocol, $cv(\hat{K}_1)$ approaches 8% at $K_1 = 0.001$, increasing to 40% for the constant infusion protocol. As the $cv(\hat{K}_1)$ for normal brain is lower for the bolus injection protocol compared to the constant infusion protocol, further presentation of results has been limited to the bolus injection protocol.

4.2.2. *Parameter estimates for bolus protocol.* Figure 6 illustrates the precision in the estimates of K_1 over the selected range of K_1 . $cv(\hat{K}_1)$ is $< 8\%$ for $K_1 > 0.001$.

4.2.3. *Count rate.* The effect of decreased injected ^{82}Rb radioactivity on the parameter estimates is illustrated in figures 7(a, b). Figure 7(a) illustrates the increase in $cv(\hat{K}_1)$ with decreasing count rate. $cv(\hat{K}_1)$ is 7.5% when $K_1 = 0.001$ and $V_p = 0.03$ for a 120 mCi

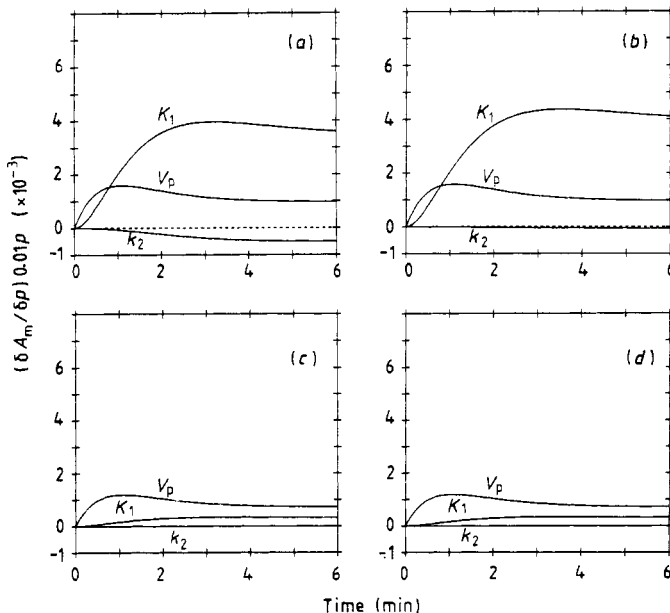


Figure 4. Sensitivity function curves for the constant infusion protocol for both tumour tissue and normal brain. Parameter values as in figure 3.

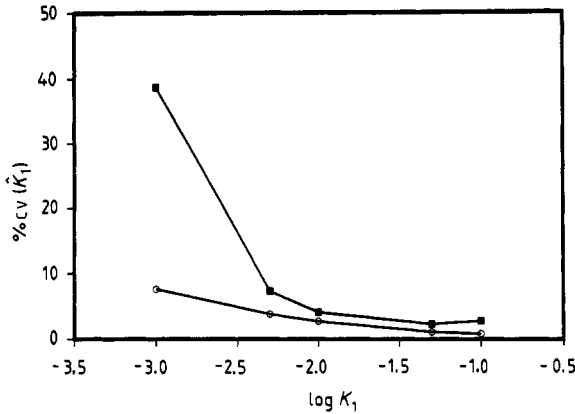


Figure 5. Comparison of bolus injection (○) and constant infusion (■) protocols. $cv(\hat{K}_1)$ is plotted as a function of K_1 for bolus and constant infusion protocols. $V_p = 0.03$, and $cv(A_m) = 5\%$. The five discrete points on each curve correspond to K_1 values of 0.1, 0.05, 0.01, 0.005 and 0.001 on a logarithmic scale.

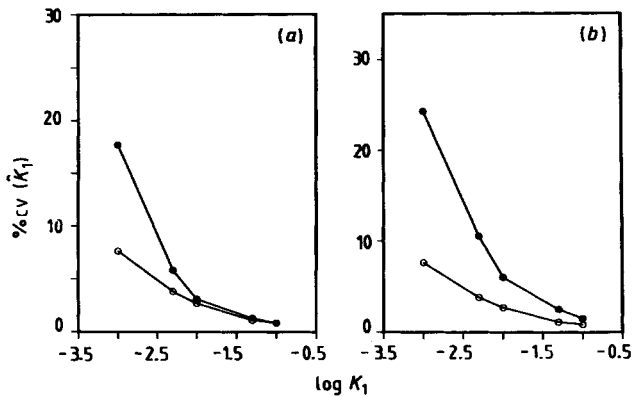


Figure 6. CV in the estimate of K_1 using the bolus injection protocol (a) $cv(\hat{K}_1)$ vs K_1 at $V_p = 0.03$ (○), 0.07 (●) when $cv(A_m) = 5\%$ and (b) $cv(\hat{K}_1)$ vs K_1 at $cv(A_m) = 5\%$ (○), 10% (●) when $V_p = 0.03$.

of ⁸²Rb injection; this $cv(\hat{K}_1)$ increases to 15% and 25% when 60 mCi and 30 mCi of ⁸²Rb are injected, respectively. The $cv(\hat{V}_p)$ also increases with decreasing count rate, increasing from 2.7% to 5.1% for injected ⁸²Rb radioactivity corresponding to 120 and 30 mCi, respectively, when $K_1 = 0.1$ and $V_p = 0.03$.

4.2.4. Tissue heterogeneity and number of scans. These two variables have a very small effect on the parameter estimates (see § 5).

5. Discussion

5.1. Sensitivity function curves

5.1.1. Bolus injection. For tumour tissue, the magnitude of the sensitivity functions for the model parameters suggests that A_m is more sensitive to changes in K_1 and V_p than

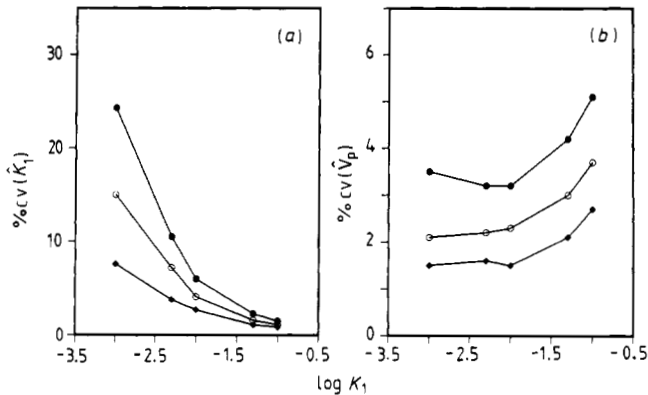


Figure 7. Effect of count rate on parameter estimates for the bolus injection protocol (a) $\text{CV}(\hat{K}_1)$ vs K_1 for three different amounts of ^{82}Rb injected (\bullet , 30; \circ , 60; \blacklozenge , 120 mCi) and (b) $\text{CV}(\hat{V}_p)$ vs K_1 for the same amounts of injected ^{82}Rb . $\text{CV}(A_m)$ is assumed to be 5%, $V_p = 0.03$.

to changes in k_2 (figure 3(a)). A_m becomes almost insensitive to changes in k_2 when $k_2 = K_1/10$ (figure 3(b)). Moreover, the shape of the SF curves suggests that A_m is most sensitive to changes in V_p during the initial phase of the study and most sensitive to changes in K_1 during the later phase of the study; K_1 becomes the dominant parameter after 1.0 min, and the effect of V_p becomes negligible by about 4 min. This difference in the shape of the SF curves for K_1 and V_p suggests that the estimates of K_1 and V_p are relatively independent. If k_2 is small (i.e. $<0.1 K_1$), K_1 and V_p can be uniquely estimated with great accuracy. For normal brain, figures 3(c, d) indicate that A_m becomes much less sensitive to changes in K_1 , and the temporal separation of the K_1 and V_p effects decreases; sensitivity of A_m to K_1 becomes dominant after about 3 min. A_m is totally insensitive to changes in k_2 over a ten-fold change, and, therefore, k_2 can be dropped from the model. Thus, for normal brain, a 6 min study will yield a good estimate of V_p and a fair estimate of K_1 , but the estimate of k_2 will be associated with very large errors.

5.1.2. Constant infusion. In the case of a constant infusion, A_m is more sensitive to changes in K_1 than to changes in V_p , and the K_1 and V_p SF curves are not as well separated as for the bolus case; V_p contributes significantly to the change in A_m until the very end of the study (figures 4(a, b)). A_m is sensitive to changes in k_2 only for large k_2 (i.e. $k_2 = K_1$). The situation, however, becomes quite different for normal brain tissue; figures 4(c, d) clearly show that A_m is less sensitive to changes in K_1 , and the temporal separation of the K_1 and V_p effects becomes less apparent. Again, k_2 can be neglected for normal brain.

5.2. Computer simulations

A comparison of bolus injection and constant infusion techniques indicates that $\text{CV}(\hat{K}_1)$ is, in fact, larger for the constant infusion protocol (figure 5), in agreement with our SF analysis. Given its technical simplicity and statistical advantages, we will therefore confine our attention to an analysis of the bolus injection protocol. Lammertsma *et al* (1984) reported a low value for back-diffusion ($k_2 < 0.02$) for a single tumour in one patient, and Yen and Budinger (1981) estimated a similar value for k_2 in their

studies of BBB disruption by 3 M urea in Rhesus monkeys. We have, therefore, further limited our discussion to the case when $k_2 = 0.1 K_1$. Computer simulations suggest that the three variables that most significantly affect the accuracy of parameter estimation are time shift (between blood and brain radioactivity curves), blood waveform distortion due to smearing and PET count rate. The effects of time shift and blood curve smearing have already been discussed (Dhawan *et al* 1988).

Figure 6 describes the error sensitivity of the bolus technique to the magnitude of V_p and $CV(A_m)$.

5.2.1. Count rate. Decrease in count rate (lower $^{82}\text{Sr}/^{82}\text{Rb}$ generator activity for the same elution speed and identical scanning protocol) increases $cv(\hat{K}_1)$, especially for $K_1 < 0.005$ (figure 7(a)). $cv(\hat{V}_p)$ increases uniformly over the whole range of K_1 , as shown in figure 7(b), but its absolute magnitude remains acceptable ($< 6\%$). A cv of $< 10\%$ in \hat{K}_1 for normal tissue, even when only 60 mCi of ^{82}Rb is injected, suggests that multiple studies can be carried out in the same subject without excessive radiation exposure (Kearfott 1982); normal brain provides an internal control for multiple studies when the effect of radiation or chemotherapy on tumour tissue is to be investigated (Jarden *et al* 1985).

Factors of minor influence on parameter estimates include tissue heterogeneity and the number of scans/scan intervals. Tissue (tumour-brain) heterogeneity did not significantly affect the $cv(\hat{K}_1)$ and $cv(\hat{V}_p)$ and this can be explained by observing that the model (equation (3)) becomes linear in K_1 and V_p if k_2 is small/negligible with respect to K_1 . Increasing the number of scans from 6 to 12 does not change the results significantly. The explanation for this lies in the fact that a double-integral model is less sensitive than a single-integral model to temporal resolution in the brain curve, as long as the blood curve changes at a fast enough rate to contain all the frequencies expected in the physiological rate constants (Budinger *et al* 1985) and is adequately sampled. As shown in figure 2(a), our blood curves were sampled at 9 s intervals, and the rate constants in the simulated blood curves (figure 2(b): a good approximation to the actual blood curve) for the bolus injection protocol are an order of magnitude smaller than K_1 or k_2 . The only absolute requirement for the scanning protocol is that there be at least one scan more than the number of parameters; each scan should contain enough counts to keep the error in A_m small (preferably $< 5\%$) and the scans should adequately sample the rapidly changing phase of the brain radioactive curve.

5.2.2. Effect of Rb uptake into red blood cells (RBCs). Using a constant infusion technique, Lammertsma *et al* (1984) reported no significant uptake of ^{82}Rb into RBC over a period of 15 min. In contrast, in five patients whose blood was repeatedly sampled during a 'slow bolus' ^{82}Rb infusion, Jarden *et al* (1985) demonstrated significant ^{82}Rb uptake. This RBC uptake can be accounted for by replacing $V_p C_p$ in the last term of equation (3) with $(V_p C_p + V_{\text{rbc}} C_{\text{rbc}})$, where C_{rbc} is the ^{82}Rb concentration in RBC and V_{rbc} is red-cell volume. Solution of the model equation will then require a well defined *in vivo* RBC ^{82}Rb uptake curve (to obtain C_{rbc}) and an accurate estimate of regional cerebral haematocrit (to obtain V_{rbc}). Given that these extra measurements will involve errors of their own, an approximation can be used if $C_p \approx C_{\text{rbc}}$ after the initial 15–30 s; the last term of equation (3) then becomes $V_b C_b$, where C_b is whole-blood radioactivity, and V_b is tissue blood volume. Strictly speaking, V_b is an 'apparent' tissue blood volume because of the initial variability in V_b before C_{rbc} approaches C_p ; also, in tumours, V_b contains a contribution from extracellular fluid (rapidly exchanging with plasma).

5.2.3. Effect of adding an irreversible compartment. $^{82}\text{Rb}/\text{PET}$ studies based on equation (3) are primarily useful for obtaining estimates of K_1 and V_p . Constant infusions of ^{82}Rb for periods in excess of 15 min are required to provide accurate estimates of k_2 and/or k_3 , but such studies may be associated with increased radiation exposure. For a 6 min study, computer simulations suggest that fitting k_3 in addition to K_1 , k_2 and V_p increases the error in K_1 (unpublished data). In order to obtain reasonable estimates of all four parameters (K_1 , k_2 , k_3 and V_p), a longer-lived radionuclide, such as ^{68}Ga , and a different scanning protocol must be employed.

Our estimates of K_1 (Jarden *et al* 1985) are similar to those derived from the data of Brooks *et al* (1984), who utilised the Rb extraction model of Lammertsma *et al* (1984). The fact that our model, which assumes the presence of backflux (i.e. $k_2 > 0$), and the model proposed by Lammertsma *et al*, which assumes that $k_2 = 0$, yield similar values for K_1 and V_p , suggests that tumour k_2 for ^{82}Rb are less than $2 \times 10^{-2} \text{ min}^{-1}$. Lammertsma's (1984) approach to the measurement of regional ^{82}Rb extraction requires three separate PET studies and is associated with an overall uncertainty of 10% for brain tumours. In contrast, our double-integral model requires a single 6 min study to obtain estimates of a unidirectional influx rate constant (K_1) and tissue plasma water volume (V_p) with a similar degree of uncertainty. The extraction fractions of Lammertsma *et al* cannot be directly compared with the unidirectional influx rate constant (K_1) in our initial publication (Jarden *et al* 1985), since we did not measure regional cerebral blood flow. However, in a subsequent series of patients with primary and metastatic brain tumours, tumour blood flow, measured in conjunction with $^{82}\text{Rb}/\text{PET}$ studies, averaged $31.5 \text{ ml min}^{-1} 100 \text{ ml}^{-1}$; computed PS products for tumour tissue ranged from 131 to $824 \times 10^{-5} \text{ ml s}^{-1} \text{ g}^{-1}$ (see part II of this paper for details). These PS products are similar to the values obtained by Brooks *et al* (1984). We agree with Lammertsma *et al* that newer PET scanners which can estimate regional count density in normal brain with a CV of approximately 5%, will, according to our simulations, allow accurate estimates of K_1 and V_p to be obtained for brain regions smaller than 25 cm^3 . Finally, the major advantage of our bolus injection protocol is the ability to rapidly acquire data in sick patients and to perform serial studies in the same patient over a period of minutes to hours, thus permitting the measurement of acute changes in blood-brain/tumour ^{82}Rb transport (or indirectly blood-brain barrier permeability), such as are likely to occur following whole-brain irradiation or corticosteroid therapy.

6. Conclusion

The reported error analysis demonstrates the feasibility of PET measurements of unidirectional blood-to-brain transport rate constants for Rb in regions of increased BBB permeability using ^{82}Rb and an intravenous bolus injection or a constant infusion protocol. Accurate estimates of tissue plasma volume, V_p , may also be obtained, but estimates of efflux rate constants are associated with large errors. The bolus injection technique has the associated benefits of technical simplicity, statistical advantages and a short study duration.

Acknowledgments

The authors wish to thank George Abramson for manuscript preparation. This work was supported in part by grants NS-23473 and NS-03346 from the National Institute of Neurological and Communicative Diseases and Stroke.

Résumé

Mesure du transport sang-cerveau et sang-tumeur du ^{82}Rb par tomographie à émission de positons. I: Analyse des erreurs et simulation par ordinateur.

Les auteurs ont estimé *in vivo* les constantes de débit de transport unidirectionnel (K_1) du sang vers le cerveau et du sang vers la tumeur pour le ^{82}Rb (période 76 secondes), ainsi que le volume d'eau plasmatique par unité de masse de tissu cérébral et tumoral (V_p) au moyen de la tomographie dynamique à émission de positons (PET). La précision de ces estimations dépend de la précision des mesures par PET de la radioactivité au niveau des régions cérébrale et tumorale, ainsi que de celle des mesures de la radioactivité contenue dans tout le sang de l'organisme au moyen d'un compteur puits à scintillations, cette dernière dépendant du temps de transit de la radioactivité dans le sang artériel. Les auteurs ont employé un modèle bicompartimental pour obtenir les estimations de k_1 , k_2 (constantes débit d'écoulement) et de V_p à partir des données PET du ^{82}Rb . Les erreurs commises au cours de l'estimation de ces paramètres ont été étudiées (1) qualitativement au moyen d'une étude de sensibilité et (2) quantitativement au moyen de simulations par ordinateur. L'effet de l'addition d'un troisième compartiment irréversible et de la valeur k_3 de sa constante de débit unidirectionnel a également été étudié. Les auteurs discutent également les avantages et les désavantages de l'injection d'un bolus, comparés à ceux d'une injection continue. Ils comparent la précision des paramètres estimés à partir des données actuelles sur patient à ceux obtenus à partir des simulations par ordinateur contenues dans la partie II de cet article.

Zusammenfassung

Positronenemissionstomographische Messungen des Blut-Gehirn- und des Blut-Tumor-Transportes von ^{82}Rb . I: Fehleranalyse und Computersimulationen.

Die in einer Richtung verlaufenden Blut-Gehirn- und Blut-Tumor-Transportgeschwindigkeitskonstanten (K_1) für ^{82}Rb (Halbwertszeit 76 s) und das Plasma-Wasser-Volumen pro Masseneinheit des Gehirn-Tumor-Gewebes (V_p) können *in vivo* mit Hilfe der Positronenemissionstomographie (PET) bestimmt werden. Die Genauigkeit dieser Bestimmung hängt ab von der Genauigkeit der PET-Messungen der regionalen Gehirn-Tumor-Aktivität, die wiederum vom Zeitverlauf der arteriellen Blutaktivität abhängt. Ein Zwei-Compartimentmodell wurde verwendet, um Werte für k_1 , k_2 (Abflußgeschwindigkeitskonstante) und V_p aus ^{82}Rb -PET-Daten abzuleiten. Die Fehler bei der Bestimmung dieser Parameter wurden qualitativ untersucht (1) durch Analyse der Sensitivitätsfunktion und quantitativ (2) mit Hilfe von Computersimulationen. Der Einfluß des Hinzuziehens eines dritten irreversiblen Compartiments und seiner in einer Richtung verlaufenden Geschwindigkeitskonstanten k_3 wurde ebenfalls untersucht. Die Vor- und Nachteile von Bolusinjektionen gegenüber kontinuierlicher Infusion werden diskutiert. Die Genauigkeit der aus aktuellen Patientendaten bestimmten Parameter wird in Teil II der vorliegenden Arbeit verglichen mit der, die man durch Computersimulationen erhält.

References

- Blasberg R G, Fenstermacher J D and Patlak C S 1983a Transport of alpha-aminoisobutyric acid across brain capillary and cellular membranes *J. Cerebr. Blood Flow Metab.* **3** 8-32
- Blasberg R G, Patlak C S and Fenstermacher J D 1983b Selection of experimental conditions for the accurate determination of blood-brain transfer constants from single time experiments: a theoretical analysis *J. Cerebr. Blood Flow Metab.* **3** 215-25
- Blasberg R G, Wright D C, Patlak C S, Brooks R A, Carson R E, Groothuis D R and DiChiro G 1984 Determination of regional blood-tissue transfer constants and initial (plasma) volume in brain and brain tumors using ^{68}Ga -EDTA and dynamic positron emission tomography *J. Nucl. Med.* **25** P51
- Brooks D J, Beaney R P, Lammertsma A A, Leenders K L, Horlock P L, Kensett M J, Marshall J, Thomas D G and Jones T 1984 Quantitative measurement of blood-brain barrier permeability using rubidium-82 and positron emission tomography *J. Cerebr. Blood Flow Metab.* **4** 535-45
- Budinger T F, Derenzo S E, Greenberg W L, Gullberg G T and Huesman R H 1978 Quantitative potentials of dynamic emission tomography *J. Nucl. Med.* **19** 309-15
- Budinger T F and Huesman R H 1985 Ten precepts for quantitative data acquisition and analysis *Circulation* **72** (suppl IV) 53-62

- Dhawan V, Jarden J O, Strother S C and Rottenberg D A 1988 Effect of blood curve smearing on the accuracy of parameter estimates obtained for ^{82}Rb /PET studies of blood-brain barrier permeability *Phys. Med. Biol.* **33** 61-74
- Hawkins R A, Phelps M E, Huang S C, Wapenski J A, Grimm P D, Parker R G, Juillard G and Greenberg P 1984 A kinetic evaluation of blood brain barrier permeability in human brain tumors with [^{68}Ga]EDTA and positron computed tomography *J. Cerebr. Blood Flow Metab.* **4** 507-15
- Herscovitch P and Raichle M E 1983 Effect of tissue heterogeneity on the measurement of cerebral blood flow with the equilibrium C^{15}O_2 inhalation technique *J. Cerebr. Blood Flow Metab.* **3** 407-15
- Huang S C and Phelps M E 1985 Error in parameter estimates with variations in flow: measurement of oxygen utilization with positron-emission tomography *Circulation* **72** (suppl IV) 77-80
- Jarden J O, Dhawan V, Kearfott K J and Rottenberg D A 1984 Measurement of blood-brain barrier permeability using ^{82}Rb and positron emission tomography *Ann. Neurol.* **16** 131
- Jarden J O, Dhawan V, Poltorak A, Posner J B and Rottenberg D A 1985 Positron emission tomographic measurement of blood-to-brain and blood-to-tumor transport of ^{82}Rb : the effect of dexamethasone and whole-brain radiation therapy *Ann. Neurol.* **18** 636-46
- Kearfott K J 1982 Radiation absorbed dose estimates for positron emission tomography (PET): K-38, Rb-81, Rb-82 and Cs-130 *J. Nucl. Med.* **23** 1128-32
- Kessler R M, Goble J C, Bird J H, Girton M E, Doppman J L, Rapoport S I and Barranger J A 1984 Measurement of blood-brain barrier permeability with positron emission tomography and [^{68}Ga]EDTA *J. Cerebr. Blood Flow Metab.* **4** 323-8
- Lammertsma A A, Brooks D J, Frackowiak R S J, Heather J D and Jones T 1984 A method to quantitate the fractional extraction of Rubidium-82 across the blood-brain barrier using positron emission tomography *J. Cerebr. Blood Flow Metab.* **4** 523-34
- Lockwood A H 1984 Functional evaluation of blood-brain barrier using positron emission tomography *Ann. Neurol.* **15** (suppl) S103-6
- Takagi S, Kenny P J and Gilson A J 1984 A quantitative method for the measurement of cerebral vascular extraction in vivo following intravenous injection: simulation studies *J. Cerebr. Blood Flow Metab.* **4** 564-73
- Yen C K and Budinger T F 1981 Evaluation of blood-brain barrier permeability changes in rhesus monkeys and man using ^{82}Rb and positron emission tomography *J. Comput. Assist. Tomogr.* **5** 792-9